DMD Fast Forward. Published on March 26, 2015 as DOI: 10.1124/dmd.115.063743
This article has not been copyedited and formatted. The final version may differ from this version.

Use of transgenic mouse models to understand the oral disposition and drug-drug interaction potential of cobimetinib, a MEK inhibitor

Edna F Choo, Sarah Woolsey, Kevin DeMent, Justin Ly, Kirsten Messick, Ann Qin, Ryan Takahashi

Genentech Inc., South San Francisco, CA 94080

DMD Fast Forward. Published on March 26, 2015 as DOI: 10.1124/dmd.115.063743
This article has not been copyedited and formatted. The final version may differ from this version.

DMD#63743

Running Title

Use of CYP transgenic mouse models

Corresponding Author

Edna F Choo, Ph.D.
Genentech, Inc.
1 DNA Way
South San Francisco, CA 94080
Phone: 650-467-3861
Fax: 650-225-6452
Email: choo.edna@gene.com

Number of Text Pages: 29
Number of Tables: 3
Number of Figures: 2
Number of References: 29
Number of Words:
Abstract: 246
Introduction: 558
Results and Discussion: 2032

List of Non-Standard Abbreviations:

CYP, Cytochrome P450; Tg, Transgenic; WT, Wild-type; Cyp3a$^{-/-}$Tg-3A4$_{Hep}$, transgenic mice with CYP3A4 in the liver only; Cyp3a$^{-/-}$Tg-3A4$_{Int}$, transgenic mice with CYP3A4 in the intestine only; Cyp3a$^{-/-}$Tg-3A4$_{Hep/Int,}$ transgenic mice with CYP3A4 in both liver and intestine; CL, clearance, CL_{int}, intrinsic clearance; F, bioavailability; F_a, fraction absorbed; F_g, Fraction escaping intestinal extraction, $F_{h,}$ Fraction escaping hepatic extraction; LC-MS/MS, liquid chromatography tandem mass spectrometry

DMD Fast Forward. Published on March 26, 2015 as DOI: 10.1124/dmd.115.063743
This article has not been copyedited and formatted. The final version may differ from this version.

ABSTRACT

Data from the clinical absolute bioavailability (F) study with cobimetinib suggested that F was lower than predicted based on its low hepatic extraction and good absorption. The CYP3A4 transgenic mouse model with differential expression of CYP3A4 in the liver ($Cyp3a^{-/-}$Tg-$3A4_{Hep}$) or intestine ($Cyp3a^{-/-}$Tg-$3A4_{Int}$) and both liver and intestine ($Cyp3a^{-/-}$Tg-$3A4_{Hep/Int}$) were used to study the contribution of intestinal metabolism to the F of cobimetinib. In addition, the effect of CYP3A4 inhibition and induction on cobimetinib exposures was tested in the $Cyp3a^{-/-}$Tg-$3A4_{Hep/Int}$ and PXR-CAR-CYP3A4/CYP3A7 mouse models, respectively. After IV administration of 1 mg/kg cobimetinib to wild-type (WT; FVB), $Cyp3a^{-/-}$Tg-$3A4_{Hep}$, $Cyp3a^{-/-}$Tg-$3A4_{Int}$ or $Cyp3a^{-/-}$Tg-$3A4_{Hep/Int}$ mice, CL (26-35 mL/min/kg) was similar in the CYP3A4 transgenic and WT mice. After oral administration of 5 mg/kg cobimetinib, the AUC of cobimetinib in WT, $Cyp3a^{-/-}$Tg-$3A4_{Hep}$, $Cyp3a^{-/-}$Tg-$3A4_{Int}$ or $Cyp3a^{-/-}$Tg-$3A4_{Hep/Int}$ mice were 1.35, 3.39, 1.04 and 0.701 μM.h, respectively. The ~80% lower AUC of cobimetinib in transgenic mice when intestinal CYP3A4 was present suggested that intestinal first pass contributed to the oral CL of cobimetinib. Oxidative metabolites observed in human circulation were also observed in the transgenic mice. In drug-drug interactions (DDI) studies using $Cyp3a^{-/-}$Tg-$3A4_{Hep/Int}$ mice, a 8- and 4-fold increase in oral and IV cobimetinib exposure, respectively, were observed with itraconazole co-administration. In PXR-CAR-CYP3A4/CYP3A7 mice, rifampin induction decreased cobimetinib oral exposure by ~80%. Collectively, these data are supportive that CYP3A4 intestinal metabolism contributed to the oral disposition of cobimetinib and suggests that under certain circumstances the transgenic model may be useful in predicting clinical DDI.

DMD Fast Forward. Published on March 26, 2015 as DOI: 10.1124/dmd.115.063743
This article has not been copyedited and formatted. The final version may differ from this version.

INTRODUCTION

Cobimetinib ((*S*)-[3,4-difluoro-2-(2-fluoro-4-iodophenylamino)phenyl] [3-hydroxy-3-(piperidin-2-yl)azetidin-1-yl]methanone hemifumarate) is a MEK inhibitor currently being tested in multiple combinations, including a completed phase 3 clinical trial in combination with vemurafenib, in patients with metastatic melanoma (Larkin et al., 2014). The pharmacokinetics of cobimetinib has been well characterized in clinical pharmacology studies in healthy subjects (Musib et al., 2013). Cobimetinib undergoes low clearance (11.7 L/h), is well absorbed (F_a ~88%; estimated from the sum of radioactivity recovered in urine (17.8%) and radioactivity in feces that was characterized as metabolites (69.9%) and has an absolute bioavailability of 45% (Musib et al., 2013). Clinical data from the absolute bioavailability study suggests that intestinal first pass metabolism may play a role in decreasing the bioavailability of cobimetinib. Indeed, analysis of the data from the absolute bioavailablity study with knowledge of F_a, suggested that the estimated intestinal first pass metabolism/extraction (E_g) of cobimetinib correlates to F whereas there was no correlation between F and hepatic extraction (E_h) (American Society of Clinical Pharmacology and Therapeutics Annual Conference, Atlanta, 2014). Consistent with this finding, data from recombinant enzymes and chemical inhibition studies in microsomes, showed that cobimetinib was metabolized by CYP3A4/5 and UGT2B7 (data on file), enzymes known to be expressed in the intestine (Shen et al., 1997; Ritter, 2007; Rowland et al., 2013).

The differences in metabolizing enzyme specificity and regulation, limit the use of animal models in directly predicting metabolism/disposition in humans (Martignoni et al., 2006). The increasing availability of “knockout-knockin” mice, where the specific mouse gene is replaced with the corresponding human gene of interest has provided the opportunity to interrogate in an in vivo setting, for example, the ability to predict a priori the role of transporters/CYP’s on a drug/compounds disposition (Scheer et al., 2008; Scheer et al., 2010; Scheer et al., 2012). Specifically, the generation of the CYP3A4 knockout and humanized CYP3A4 mice with differential expression of CYP3A4 in the intestine or liver or in both the intestine or liver provide an attractive tool to investigate the contribution of each organ to a compounds/drug disposition. For example, van Herwaarden et al., 2007 (van Herwaarden et al., 2007), have shown using these mice the contribution of intestinal first pass metabolism and/or P-gp efflux on the disposition of docetaxel. In addition, van Waterschoot, et al., 2009 (van Waterschoot et al., 2009a), using these same mice, was able to show the contribution of intestinal CYP3A4 on oral triazolam exposure and an increase in triazolam exposure when co-administered with the CYP3A inhibitor, ketoconazole. Other models that have been used to determine the contribution of hepatic vs. intestinal metabolism to the oral disposition of a drug/compound for instance include: isolated perfused organ systems (preclinical); administration of compound/drug at different regions of the gut with or without local inhibition by CYP3A inhibitors; administration of drug during the anhepatic phase of human during liver transplantation, etc.

DMD Fast Forward. Published on March 26, 2015 as DOI: 10.1124/dmd.115.063743
This article has not been copyedited and formatted. The final version may differ from this version.

The purpose for conducting the studies reported here were to: 1) test our hypotheses that cobimetinib undergoes intestinal first pass metabolism, utilizing the transgenic with differential expression CYP3A4 mice in the intestine ($Cyp3a^{-/-}$Tg-$3A4_{Int}$), liver ($Cyp3a^{-/-}$ Tg-$3A4_{Hep}$), or intestine and liver ($Cyp3a^{-/-}$Tg-$3A4_{Hep/Int}$); 2) determine the utility of the transgenic mice with intestinal and liver expression of CYP3A4 to predict the DDI effect of CYP3A inhibition by itraconazole and 3) determine if the PXR-CAR-CYP3A4/CYP3A7 mice could to predict the clinical effect of rifampin induction on the exposure of cobimetinib.

DMD Fast Forward. Published on March 26, 2015 as DOI: 10.1124/dmd.115.063743
This article has not been copyedited and formatted. The final version may differ from this version.

MATERIALS AND METHODS

Animals

FVB (wild-type), Cyp3a knockout (KO), CYP3A4 transgenic mice with mouse Cyp3a deleted and replaced with human CYP3A4 in the liver ($Cyp3a^{-/-}Tg\text{-}3A4_{Hep}$), intestine ($Cyp3a^{-/-}Tg\text{-}3A4_{Int}$) or liver and intestine ($Cyp3a^{-/-}Tg\text{-}3A4_{Hep/Int}$) were obtained from Taconic, New York. PXR-CAR-CYP3A4/3A7 mice were obtained from Taconic; Artemis, Germany. All animals were female, 8-10 weeks old at the time of study and weighed between 20 to 25 g. In all studies, serial blood samples (20 μL) were collected by tail nick at 0.25, 0.5, 1, 3, 6, 8, and 24 h post-dose. All animals studies were carried out in accordance with the Guide for the Care and Use of Laboratory Animals as adopted and promulgated by the U.S. National Institutes of Health, and were approved by the Institution's Animal Care and use Committee.

Determining Contribution of Intestinal and Hepatic CYP3A4 in Mice

Animals (n=3 female mice for transgenic group; n=6 female for FVB group) were dosed with cobimetinib 1 mg/kg IV (in phosphate buffered saline) or 5 mg/kg orally (suspended in 0.5% methylcellulose/0.2% Tween (MCT)). In addition to PK analysis, terminal plasma samples were collected from n=2 animals after IV and PO dosing for metabolite determination at 1 and 3 h post cobimetinib dosing.

Effect of CYP3A4 Inhibition or Induction on Cobimetinib Exposure in Mice

The effect of CYP3A4 inhibition was determined in $Cyp3a^{-/-}Tg\text{-}3A4_{Hep/Int}$, FVB and Cyp3a KO mice (n=3 female mice each) administered itraconazole ($Sporanox^{R}$) 100

mg/kg PO daily for 4 days prior to cobimetinib administration. On the 4th day, cobimetinib (5 mg/kg PO or 1 mg/kg IV) was administered 30 min after the last dose of itraconazole. Induction of CYP3A4 was tested in humanized PXR-CAR-CYP3A4/3A7, where rifampin (10 mg/kg PO, n=3) or vehicle (n=3) were dosed daily for 5 days. On the 5th day, cobimetinib (5 mg/kg PO) was dosed 1 h after the last dose of rifampin. PK samples were collected as described above and concentrations of cobimetinib and itraconazole or rifampin were determined.

LC-MS/MS Analysis

Concentrations of cobimetinib were determined by a non-validated liquid chromatography tandem mass spectrometry (LC-MS/MS) assay. The plasma samples were prepared for analysis by placing a 25 µL aliquot into a 96-well plate followed by the addition of 5 µL of internal standard ($^{6}C_{13}$ analogue of cobimetinib, 2µg/mL in 50:50, v:v, DMSO:water) and 200 µL acetonitrile. The samples were vortexed and centrifuged at 1600 g for 15 min at room temperature, 50µL of the supernatant was diluted with 150 µL of water and 5 µL of the solution was injected onto an analytical column. A SIL-30ACMP autosampler system (Shimadzu, Columbia MD) was linked to LC-30AD pumps (Shimadzu, Columbia MD), coupled with an API 5500 Qtrap mass spectrometer (AB Sciex, Foster City, CA) for sample analysis. The aqueous mobile phase was water with 0.1% formic acid (A) and the organic mobile phase was acetonitrile with 0.1% formic acid (B). The gradient was as follows: starting at 25% B and increased to 95% B for 0.6 min, maintained at 95% B for 0.1 min, then decreased to 25% B within 0.1 min. The total flow rate was 1.4 mL/min and samples were injected onto a Kinetex XB C-18

(30 X 2.1 mm, 2.6 µm) analytical column (Phenomenex, Torrance, CA) with a total run time of 0.8 minutes. Data was acquired using multiple reaction monitoring (MRM) in positive ion electrospray mode with an operating source temperature of 600°C. The transition used for cobimetinib and internal standard ($^{6}C_{13}$ cobimetinib) was *m/z* 532.0 → 249.2 and 538.0 → 255.2, respectively. The lower and upper limits of quantitation of the assay for cobimetinib were 0.002 µM and 37.7 µM.

Pharmacokinetic Analysis

Pharmacokinetic (PK) parameters were calculated by non-compartmental methods as described in Gibaldi and Perrier (Gibaldi and Perrier, 1982) using Phoenix™ WinNonlin®, version 6.3.0 (Pharsight Corporation, Mountain View, CA) All PK parameters are presented as mean ± standard deviation (SD).

In vitro Metabolism Studies

Pooled human liver microsomes were obtained from BD Gentest (San Jose, CA; catalog #452117). Liver microsomes from FVB, Cyp3a$^{-/-}$ or Cyp3a$^{-/-}$Tg-3A4$_{Hep/Int}$ mice were freshly prepared from individual livers using a modification of the method described by Hill (Hill, 2004). Briefly, tissues were homogenized in 4 volumes of homogenization buffer using an Omni Bead Ruptor 24 (Omni International, Kennesaw, GA). S9 fraction was prepared by centrifugation at 9000 g for 20 min at 4°C, and microsomes were isolated via ultracentrifugation. Following optimization for conditions, final incubation conditions included 1 µM cobimetinib, 0.05 mg/mL liver microsomal protein, and an incubation time-course (5 time points) of 20 min. Incubations were conducted in

triplicate/timepoint in in 100 mM KH_2PO_4 buffer (pH 7.4) containing 1 mM $MgCl_2$, cobimetinib (1 µM) and initiated with NADPH (1 mM) in a total incubation volume of 0.1 mL. The reactions were terminated by the addition of 2 volumes of acetonitrile containing 25 ng/ml of $^{13}C_6$- cobimetinib as internal standard. The concentration of cobimetinib remaining was measured via LC-MS/MS analysis. The in vitro intrinsic clearance in the units of µL/min/mg microsomal protein was calculated utilizing the in vitro half-life approach described by Obach et al. (Obach et al., 1997). Scaling to whole body CL were conducted using the "well stirred" model described by Wilkinson and Shand (Wilkinson and Shand, 1975) and previously reported physiological parameters for mouse and human (Davies and Morris, 1993).

Metabolite Confirmation

Three previously identified circulating human oxidative metabolites of cobimetinib (Takahashi et., al., manuscript in preparation) were monitored by LC-MS/MS (M12, M18 and M19; see supplementary Figure S1). Plasma collected at 1 and 3 h post cobimetinib dosing from transgenic mice were extracted with acetonitrile and the supernatants were concentrated under vacuum and injected to the LC column. Cobimetinib and its metabolites were eluted from a Kinetex PFP 50×2.1 mm, 2.6 µm column (Phenomenex, Torrance, CA) with mobile phases of 0.1% formic acid in water and acetonitrile. Metabolites were measured using multiple reaction monitoring (MRM) with a 5500 QTrap equipped with a TurboIonSpray interface (AB Sciex, Foster City, CA). In positive mode, the following analytes and MRM (546.0→249) were monitored: M12, M18, M19

Statistical Analysis

Data in all experiments were represented as mean ± SD. Comparisons between two groups were made using an unpaired *t* test. One-way analysis of variance, followed by Bonferroni's / Dunnett's multiple comparisons test, was used to compare multiple groups. GraphPad Prism was used for all statistical analysis (version 5.00 for Mac OS X, GraphPad Software, San Diego, CA), $P<0.05$ was considered to be statistically significant.

DMD Fast Forward. Published on March 26, 2015 as DOI: 10.1124/dmd.115.063743
This article has not been copyedited and formatted. The final version may differ from this version.

RESULTS AND DISCUSSION

After IV administration of 1 mg/kg cobimetinib to WT (FVB), Cyp3a$^{-/-}$Tg-3A4$_{Hep}$, Cyp3a$^{-/-}$Tg-3A4$_{Int}$ or Cyp3a$^{-/-}$Tg-3A4$_{Hep/Int}$ mice, CL ranged from 26-35 mL/min/kg, representing 35-50% of liver blood flow (blood to plasma ratio in mice ~1.2)(Table 1). The data suggested that IV CL were not significantly different in WT, CYP3A4 transgenic and Cyp3a$^{-/-}$ animals. In Cyp3a$^{-/-}$ animals the CL of cobimetinib was 20.8 mL/min/kg (Table 1), suggesting the involvement of nonCyp3a metabolizing enzymes in the CL of cobimetinib (based on ^{14}C ADME studies in rat, dog and human cobimetinib is also likely to be extensively metabolized in mouse; Takahashi et., al., Manuscript in preparation). In contrast to the IV study where similar CL was observed across mice, after oral administration of 5 mg/kg cobimetinib, the AUC of cobimetinib in WT, Cyp3a$^{-/-}$Tg-3A4$_{Hep}$, Cyp3a$^{-/-}$Tg-3A4$_{Int}$ or Cyp3a$^{-/-}$Tg-3A4$_{Hep/Int}$ were significantly different; 1.35, 3.39, 1.04 and 0.701 μM.h, respectively (Table 1). The up to 80% lower exposures of cobimetinib observed in animals with intestinal expression of CYP3A4 compared to mice with only hepatic expression suggested that intestinal CYP3A4 played a major role in the oral disposition of cobimetinib. This finding was similar to the observation with docetaxel (van Herwaarden et al., 2007) and triazolam (van Waterschoot et al., 2009a) where intestinal CYP3A4 had a major impact on oral exposure of these drugs (7.5- and 2-fold lower AUC in mice with intestine only vs. liver only expression of CYP3A4, for docetaxel and triazolam, respectively).

In Cyp3a$^{-/-}$Tg-3A4$_{Hep/Int}$ mice, the fraction escaping intestinal extraction (F_g) was estimated to be 0.23; where F = Fa*Fg*Fh (F = 0.14, F_h = 0.61 and F_a was assumed to be

DMD Fast Forward. Published on March 26, 2015 as DOI: 10.1124/dmd.115.063743
This article has not been copyedited and formatted. The final version may differ from this version.

1; Table 1). In the clinical absolute bioavailability study, F was reported to be 46.2%, F_h = 0.87 (based on a CL of 11.7 L/h and liver blood flow of 20.7 mL/min/kg). In mouse, assuming a F_a of 1 (F_a in human was estimated to be 0.88; manuscript in preparation), F_g is estimated to be 0.63 (Musib et al., 2013). Thus, F, F_g and F_h observed in the CYP3A4 transgenic mice were quantitatively different from that in human. This was not unexpected as there are physiological differences, e.g., blood flow, between species. If however, accounting for the involvement of nonCyp3a metabolism observed in CYP3a KO animals (subtracting the hepatic extraction in CYP3a KO mice which was ~0.2), F in the transgenic animals would be higher and in the range observed in human.

From in vitro incubations of cobimetinib in human liver microsomes (HLM), WT, Cyp3a$^{-/-}$ and Cyp3a$^{-/-}$Tg-3A4$_{Hep/Int}$ mouse liver microsomes (MLM) CL_{int} were 173 ± 55, 248 ± 57, 129 ± 33 and 305 ± 60 µL/min/mg protein, respectively. The CL_{int} from WT and Cyp3a$^{-/-}$Tg-3A4$_{Hep/Int}$ MLM rank ordered and scaled (incorporating plasma protein and microsomal binding; fu plasma 0.036 and fu microsome 0.48; determine by the Austin calculation (Austin et al., 2002)) the in vivo CL observed in the respective mice (Table 1). These in vitro data infers that the 9-fold difference of PO exposure in WT, Cyp3a$^{-/-}$ and Cyp3a$^{-/-}$Tg-3A4$_{Hep/Int}$ transgenic mice are likely to be from intestinal metabolism (Table 1) and not from hepatic CL.

Recently, the use of CYP3A4 transgenic mice to predict the CL of CYP3A4 substrates in human had been reported (Mitsui et al., 2014). Using 6 CYP3A4 substrates, the in vitro intrinsic CL from human and CYP3A4 transgenic mouse liver microsomes were reported

to be within 2-fold of each other. However, in vivo CL observed in transgenic mice could not be extrapolated directly to predict human CL. A prediction within 2-fold was only obtained from the regression of hepatic CL_{int} (back calculated from in vivo CL using the dispersion model) between human and transgenic mouse (Mitsui et al., 2014). Thus, a priori, a regression would have to be established for model compounds before human CL predictions could be made using data from transgenic mice. Although not discussed by the authors, it is worth noting, that hepatic extraction, derived from transgenic mouse and human were within 2-fold. It appears at this point that the direct utility of using transgenic mice in predicting human CL remains unclear.

To verify the relevance of the CYP3A4 transgenic mouse model we sought to determine if the circulating oxidative metabolites of cobimetinib (albeit minor; each <5% of total radioactivty in plasma, Takahashi et., al., Manuscript in preparation) in human were also observed in the transgenic mice. Indeed in the CYP3A4 transgenic mice, oxidative metabolites observed in human circulation (M12, M18, M19) were observed (see Supplemental Figure S1-A for structures). This provided supportive information that the metabolic pathways in the transgenic mice reflected those in human (which was CYP3A4 mediated; Ryan Takahashi, manuscript in preparation). M12 and M19 were also observed in plasma of FVB and Cyp3a(-/-) mice (see Supplemental Figure S1-B), the presence of human metabolites in the FVB and Cyp3a(-/-) mice was not unexpected *per se* as mouse Cyp isoforms (Cyp3a or other Cyp) have the capability to metabolize and produce the same metabolites as human. Of note, however, was that in the transgenic mice with differential liver/intestinal expression of CYP3A4, there appeared to be quantitative and

selective differences in metabolite profile. M12 levels were higher in transgenic mice expressing intestinal CYP3A4 and M18 was only observed in transgenic mice expressing liver CYP3A4. In addition, M18 was only observed where human CYP3A4 is expressed. Collectively, this data suggest that the transgenic mice provide a unique metabolite profile (compared to WT and Cyp3a(-/-)), representative (at least qualitatively) of human metabolites (see Supplemental Figure S1).

To further assess the utility of the transgenic mice, DDI studies were conducted in Cyp3a$^{-/-}$Tg-3A4$_{Hep/Int}$ and in humanized PXR-CAR-CYP3A4/3A7 mice. In Cyp3a$^{-/-}$Tg-3A4$_{Hep/Int}$ mice, inhibition of CYP3A4 by itraconazole resulted in a 8.3-fold increase in cobimetinib AUC and ~3-fold increase in C_{max} after oral administration of cobimetinib (Table 2). In addition, IV administration of cobimetinib with itraconazole (oral) resulted in ~4-fold increase in cobimetinib AUC and half-life, this is in keeping with a similar magnitude decrease in CL (Table 2). The greater DDI effect (~8- vs. ~4-fold) observed after oral dosing of cobimetinib was consistent with the contribution of intestinal CYP3A4 to the CL of cobimetinib. This finding was similar to the clinical observation reported where a greater DDI effect was observed after oral vs. IV administration of midazolam with the CYP3A inhibitor clarithromycin. A 7- and 2.7-fold increase in the exposure (AUC) of midazolam were observed after oral and IV administration, respectively (Gorski et al., 1998).

Itraconazole did not significantly alter the exposure of cobimetinib in Cyp3a KO animals, suggesting that in mice only the Cyp3a isoenzyme was inhibited by itraconazole (Table

3). In addition, itraconazole co-administration to FVB (WT) mice resulted in a 5.8-fold increase in oral exposure of cobimetinib (within the range of fold increase observed in transgenic mice; Table 3). This is consistent with the suggestion that Cyp3a enzymes in mice may be the primary enzyme that metabolizes cobimetinib (Table 3). Collectively this data suggests that the magnitude increase in CL of cobimetinib from co-administration with itraconazole to Cyp3a$^{-/-}$Tg-3A4$_{Hep/Int}$ mice was higher than expected based on the apparent low CYP3A4 contribution to CL of cobimetinib (~ 30% difference in CL between Cyp3a(-/-) vs. transgenic animals; Table 1) and the specificity of itraconazole to inhibition of only Cyp3a. The reason for the higher than expected decrease in cobimetinib CL when co-administered with itraconazole is unclear. Of note, systemic exposure of itraconazole in this studies was similar to clinical exposures from a dose of 200 mg Sopranox^{R} solution (Sopranox^{R} Product Insert and Supplemental Figure S2), however the intestinal/hepatic exposures of itraconazole are unknown and may be higher than clinical tissue exposures based on the higher mg/kg dose.

In addition to studying the effect of CYP3A4 inhibition, using the PXR-CAR-CYP3A4/3A7 mice the effect of induction was investigated. It has been reported that the PXR-CAR-CYP3A4/3A7 model displays human-like CYP3A4 induction to various PXR inducers (Hasegawa et al., 2011). In addition to an increase in CYP3A4 mRNA levels after rifampin induction in PXR-CAR-CYP3A4/3A7 mice, in vivo exposures of triazolam were reported to be decreased by up to 90% after rifampin treatment (Hasegawa et al., 2011). Consistent with the role of CYP3A4 in the metabolism of cobimetinib, CYP3A4 induction resulted in ~80% decrease in the exposure of

cobimetinib (Table 2). As a reference, clinical induction of CYP3A from 600 mg of rifampin has been reported to decrease the exposure of the prototypical CYP3A substrate, midazolam by ~90-98% (Backman et al., 1996; Gorski et al., 2003); (University of Washington Drug Interaction Database). Thus, the observed effect of rifampin induction on cobimetinib in PXR-CAR-CYP3A4/3A7 mice was on the lower end of the scale compared to a sensitive CYP3A4 substrate such as midazolam. Worth noting, the exposure of rifampin in this study was consistent with clinical concentrations observed from a dose of 600 mg (Kwara et al., 2014); (see Supplementary Figure S2).

The utility of a specific transgenic model is dependent on the disposition and metabolism of the compound/drug of interest. For instance, since cobimetinib was predominantly metabolized by CYP3A4, and was metabolized by both intestinal and liver CYP3A, the CYP3A4 transgenic mice with differential expression in each tissue was an ideal model. It appeared that unlike midazolam, where mice Cyp2c metabolized midazolam and confounded the interpretation of data from Cyp3a KO mice (van Waterschoot et al., 2008), cobimetinib disposition and metabolism appeared to be mainly driven by Cyp3a/CYP3A in mice and human. However, some contribution from CYP (as evidenced by the Cyp3a KO data) and nonCYP enzymes such as UGT (fm likely to be low) on the metabolism of cobimetinib cannot be excluded. One consideration when using this model is that for some CYP3A substrates, the contribution of CYP3A5 to the metabolism of a compound can be substantial(Lamba et al., 2002). While cobimetinib appears to be mainly metabolized by CYP3A4 (data on file), for midazolam, vincristine and atanazavir, CYP3A5 has been reported to contribute to ~50-80% to the overall f_m

CYP3A (Walsky et al., 2012; Tseng et al., 2014). Therefore data generated in the CYP3A4 transgenic mice, while representative of the *3/**3 genotype (with low/no CYP3A5 expression) may not reflect the population expressing CYP3A5 (*1/*3 or *1/**1). The allelic frequency of CYP3A5*1/*3 in Caucasians and African Americans was reported to be ~17% and 40%, respectively and for CYP3A5*1/*1, ~1% and 45% in Caucasian and African American subjects, respectively. Significant ethnic variability in allelic frequency was reported (Xie et al., 2004)). In addition, many compounds/drugs are metabolized by multiple enzymes and may be substrates of transporters, thus, compensation from deletion of one enzyme, may result in compensatory increase in another metabolizing enzyme or transporter. For instance, an increase in Cyp2c55 expression is reported with deletion of Cyp3a (van Waterschoot et al., 2009b). We had characterized some of the Cyp, Ugt and transporter changes by RT-PCR and observed some changes in Cyp, transporter and Ugt expression (compared to WT animals) in both hepatic and intestinal/ duodenal tissue (see Supplemental, Figure S3 and S4). In most cases these changes were modest and unlikely to affect the overall interpretation of data for cobimetinib.

Overall, the findings from this study, albeit with one compound suggests that the transgenic mouse model under specific conditions may be a useful tool to predict the relative contribution of hepatic and intestinal metabolism. Recently, the clinical interaction data of cobimetinb with itraconazole DDI study was reported. A 6.7- and 3.2-fold increase in cobimetinib AUC and C_{max} was observed (American Society of Clinical Pharmacology and Therapeutics Annual Conference, New Orleans 2015). In addition,

based on the observed DDI data with itraconazole, a PBPK model was developed and used to simulate the effect of rifampin induction (600 mg daily). An 83% decrease in cobimetinib exposure was predicted with rifampin induction. Comparison of the observed/predicted clinical DDI data to the effect of itraconazole and rifampin in the transgenic mouse models suggests that the transgenic model provided a good prediction of the clinical DDI effect. In the future, as more data using transgenic mice becomes available, particularly for drugs in which clinical DDI and or clinical disposition is well understood, it is anticipated that in tandem with in vitro data, PBPK modeling and simulations a clearer picture of the utility and limitations of the transgenic model will become evident.

AUTHORSHIP CONTRIBUTIONS

Participated in research design: Choo, Woolsey, DeMent, Ly, Takahashi

Conducted experiments: Messick, Woolsey, DeMent, Takahashi, Qin

Contributed new reagents: Takahashi, DeMent

Performed data analysis: Choo, Woolsey, DeMent, Ly, Takahashi

Wrote or contributed to the writing of the manuscript: Choo, Woolsey, DeMent, Ly, Takahashi

REFERENCES

Austin RP, Barton P, Cockroft SL, Wenlock MC, and Riley RJ (2002) The influence of nonspecific microsomal binding on apparent intrinsic clearance, and its prediction from physicochemical properties. *Drug Metab Dispos* **30:**1497-1503.

Backman JT, Olkkola KT, and Neuvonen PJ (1996) Rifampin drastically reduces plasma concentrations and effects of oral midazolam. *Clin Pharmacol Ther* **59:**7-13.

Davies B and Morris T (1993) Physiological parameters in laboratory animals and humans. *Pharm Res* **10:**1093-1095.

Gibaldi M and Perrier D (1982) *Pharmacokinetics*. Marcel Dekker, New York.

Gorski JC, Jones DR, Haehner-Daniels BD, Hamman MA, O'Mara EM, Jr., and Hall SD (1998) The contribution of intestinal and hepatic CYP3A to the interaction between midazolam and clarithromycin. *Clin Pharmacol Ther* **64:**133-143.

Gorski JC, Vannaprasaht S, Hamman MA, Ambrosius WT, Bruce MA, Haehner-Daniels B, and Hall SD (2003) The effect of age, sex, and rifampin administration on intestinal and hepatic cytochrome P450 3A activity. *Clin Pharmacol Ther* **74:**275-287.

Hasegawa M, Kapelyukh Y, Tahara H, Seibler J, Rode A, Krueger S, Lee DN, Wolf CR, and Scheer N (2011) Quantitative prediction of human pregnane X receptor and cytochrome P450 3A4 mediated drug-drug interaction in a novel multiple humanized mouse line. *Mol Pharmacol* **80:**518-528.

Hill JR (2004) In vitro drug metabolism using liver microsomes. *Curr Protoc Pharmacol* **Chapter 7:**Unit7 8.

Kwara A, Cao L, Yang H, Poethke P, Kurpewski J, Tashima KT, Mahjoub BD, Court MH, and Peloquin CA (2014) Factors associated with variability in rifampin plasma pharmacokinetics and the relationship between rifampin concentrations and induction of efavirenz clearance. *Pharmacotherapy* **34:**265-271.

Lamba JK, Lin YS, Schuetz EG, and Thummel KE (2002) Genetic contribution to variable human CYP3A-mediated metabolism. *Adv Drug Deliv Rev* **54:**1271-1294.

Larkin J, Ascierto PA, Dreno B, Atkinson V, Liszkay G, Maio M, Mandala M, Demidov L, Stroyakovskiy D, Thomas L, de la Cruz-Merino L, Dutriaux C, Garbe C, Sovak MA, Chang I, Choong N, Hack SP, McArthur GA, and Ribas A (2014) Combined Vemurafenib and Cobimetinib in BRAF-Mutated Melanoma. *N Engl J Med* **371:**1867-1876.

Martignoni M, Groothuis GM, and de Kanter R (2006) Species differences between mouse, rat, dog, monkey and human CYP-mediated drug metabolism, inhibition and induction. *Expert Opin Drug Metab Toxicol* **2:**875-894.

Mitsui T, Nemoto T, Miyake T, Nagao S, Ogawa K, Kato M, Ishigai M, and Yamada H (2014) A useful model capable of predicting the clearance of cytochrome 3A4 (CYP3A4) substrates in humans: validity of CYP3A4 transgenic mice lacking their own Cyp3a enzymes. *Drug Metab Dispos* **42:**1540-1547.

Musib L, Choo E, Deng Y, Eppler S, Rooney I, Chan I, and Dresser MJ (2013) Absolute Bioavailability and Effect of Formulation Change, Food or Elevated pH With Rabeprazole on Cobimetinib Absorption in Healthy Subjects. *Mol Pharm.*

Obach RS, Baxter JG, Liston TE, Silber BM, Jones BC, MacIntyre F, Rance DJ, and Wastall P (1997) The prediction of human pharmacokinetic parameters from preclinical and in vitro metabolism data. *J Pharmacol Exp Ther* **283:**46-58.

Ritter JK (2007) Intestinal UGTs as potential modifiers of pharmacokinetics and biological responses to drugs and xenobiotics. *Expert Opin Drug Metab Toxicol* **3:**93-107.

Rowland A, Miners JO, and Mackenzie PI (2013) The UDP-glucuronosyltransferases: their role in drug metabolism and detoxification. *Int J Biochem Cell Biol* **45:**1121-1132.

Scheer N, Kapelyukh Y, Chatham L, Rode A, Buechel S, and Wolf CR (2012) Generation and characterization of novel cytochrome P450 Cyp2c gene cluster knockout and CYP2C9 humanized mouse lines. *Mol Pharmacol* **82:**1022-1029.

Scheer N, Ross J, Kapelyukh Y, Rode A, and Wolf CR (2010) In vivo responses of the human and murine pregnane X receptor to dexamethasone in mice. *Drug Metab Dispos* **38:**1046-1053.

Scheer N, Ross J, Rode A, Zevnik B, Niehaves S, Faust N, and Wolf CR (2008) A novel panel of mouse models to evaluate the role of human pregnane X receptor and constitutive androstane receptor in drug response. *J Clin Invest* **118:**3228-3239.

Shen DD, Kunze KL, and Thummel KE (1997) Enzyme-catalyzed processes of first-pass hepatic and intestinal drug extraction. *Adv Drug Deliv Rev* **27:**99-127.

Tseng E, Walsky RL, Luzietti RA, Jr., Harris JJ, Kosa RE, Goosen TC, Zientek MA, and Obach RS (2014) Relative contributions of cytochrome CYP3A4 versus CYP3A5

for CYP3A-cleared drugs assessed in vitro using a CYP3A4-selective inactivator (CYP3cide). *Drug Metab Dispos* **42:**1163-1173.

van Herwaarden AE, Wagenaar E, van der Kruijssen CM, van Waterschoot RA, Smit JW, Song JY, van der Valk MA, van Tellingen O, van der Hoorn JW, Rosing H, Beijnen JH, and Schinkel AH (2007) Knockout of cytochrome P450 3A yields new mouse models for understanding xenobiotic metabolism. *J Clin Invest* **117:**3583-3592.

van Waterschoot RA, Rooswinkel RW, Sparidans RW, van Herwaarden AE, Beijnen JH, and Schinkel AH (2009a) Inhibition and stimulation of intestinal and hepatic CYP3A activity: studies in humanized CYP3A4 transgenic mice using triazolam. *Drug Metab Dispos* **37:**2305-2313.

van Waterschoot RA, Rooswinkel RW, Wagenaar E, van der Kruijssen CM, van Herwaarden AE, and Schinkel AH (2009b) Intestinal cytochrome P450 3A plays an important role in the regulation of detoxifying systems in the liver. *Faseb J* **23:**224-231.

van Waterschoot RA, van Herwaarden AE, Lagas JS, Sparidans RW, Wagenaar E, van der Kruijssen CM, Goldstein JA, Zeldin DC, Beijnen JH, and Schinkel AH (2008) Midazolam metabolism in cytochrome P450 3A knockout mice can be attributed to up-regulated CYP2C enzymes. *Mol Pharmacol* **73:**1029-1036.

Walsky RL, Obach RS, Hyland R, Kang P, Zhou S, West M, Geoghegan KF, Helal CJ, Walker GS, Goosen TC, and Zientek MA (2012) Selective mechanism-based inactivation of CYP3A4 by CYP3cide (PF-04981517) and its utility as an in vitro

tool for delineating the relative roles of CYP3A4 versus CYP3A5 in the metabolism of drugs. *Drug Metab Dispos* **40:**1686-1697.

Wilkinson GR and Shand DG (1975) Commentary: a physiological approach to hepatic drug clearance. *Clin Pharmacol Ther* **18:**377-390.

Xie HG, Wood AJ, Kim RB, Stein CM, and Wilkinson GR (2004) Genetic variability in CYP3A5 and its possible consequences. *Pharmacogenomics* **5:**243-272.

DMD Fast Forward. Published on March 26, 2015 as DOI: 10.1124/dmd.115.063743
This article has not been copyedited and formatted. The final version may differ from this version.

FIGURE LEGENDS

Figure 1: A) Chemical structure of cobimetinib; B) Comparison of cobimetinib CL (Mean ± SD; n=3-6) after IV administration and C) Oral exposures (AUC; Mean ± SD, n= 3-6) of cobimetinib in FVB (wild-type), Cyp3a knock-out (KO), $Cyp3a^{-/-}$Tg-$3A4_{Hep}$, $Cyp3a^{-/-}$Tg-$3A4_{Int}$ or $Cyp3a^{-/-}$Tg-$3A4_{Hep/Int}$ mice

Figure 2: A) Cobimetinib concentration-time profiles in $Cyp3a^{-/-}$Tg-$3A4_{Hep/Int}$ mice after A) oral administration of cobimetinib (5 mg/kg, n=3) with or without co-administration with itraconazole and; B) after IV administration of cobimetinib (1 mg/kg, n=3) with or without co-administration with itraconazole (log scale)

TABLES

Table 1: Pharmacokinetic parameters of cobimetinib observed in FVB (wild-type; n=6), CYP3a knock-out (KO; n=3) and CYP3A4 transgenic mice (n=3) after IV (1 mg/kg) and oral (5 mg/kg) administration of cobimetinib.

Mouse Type/PK Parameters	FVB	Cyp3a(-/-)	Cyp3a$^{-/-}$Tg-3A4$_{Hep}$	Cyp3a$^{-/-}$Tg-3A4$_{Int}$	Cyp3a$^{-/-}$Tg-3A4$_{Hep/Int}$
			IV		
CL (mL/min/kg)	28.2 ± 4.4	20.8 ± 2.6	30.7 ± 4.6	25.9 ± 1.1	34.8 ± 12.5
Vss (L/kg)	15.3 ± 3.5	10.4 ± 0.9	12.2 ± 1.7	16.0 ± 1.0	13.8 ± 7.6
$t_{1/2}$ (hr)	7.52 ± 3.02	6.14 ± 1.38	4.96 ± 0.37	7.94 ± 0.67	5.09 ± 1.93
E	0.313 ± 0.048	0.231 ± 0.029	0.341 ± 0.051	0.288 ± 0.012	0.386 ± 0.138
F_H	0.687 ± 0.048	0.769 ± 0.029	0.659 ± 0.051	0.712 ± 0.012	0.614 ± 0.138
			PO		
AUC (μM.h)	1.38 ± 0.25	6.42 ± 1.07[a]	3.39 ± 1.43[b]	1.04 ± 0.11[c]	0.701 ± 0.087[c]
C_{max} (μM)	0.175 ± 0.041	0.479 ± 0.077	0.372 ± 0.148	0.080 ± 0.011	0.107 ± 0.011
F (%)	29	84	65	17	14

Cyp3a$^{-/-}$Tg-3A4$_{Hep}$ – liver only expression of CYP3A4; Cyp3a$^{-/-}$Tg-3A4$_{Int}$ – intestine only expression of CYP3A4; Cyp3a$^{-/-}$Tg-3A4$_{Hep/Int}$ – liver and intestinal expression of CYP3A4

[a]P<0.05 compared to FVB; [b] P<0.05 compared to Cyp3a KO; [c] P<0.05 compared to Cyp3a KO and Cyp3a$^{-/-}$Tg-3A4$_{Hep}$

DMD Fast Forward. Published on March 26, 2015 as DOI: 10.1124/dmd.115.063743
This article has not been copyedited and formatted. The final version may differ from this version.

Table 2: Affect of inhibitors (itraconazole) and inducers (rifampin) of CYP3A on the pharmacokinetics and exposure (Mean ± SD; n= 3-6/group) of cobimetinb in $Cyp3a^{-/-}$Tg-$3A4_{Hep/Int}$ and PXR-CAR-CYP3A4/3A7 mice.

	Itraconazole Study		Rifampin Study	
	No Treatment	Intraconzole	Vehicle	Rifampin
	$Cyp3a^{-/-}$Tg-$3A4_{Hep/Int}$		PXR-CAR-CYP3A4/3A7	
PO Cobimetinib				
$AUC_{(0\text{-}tlast)}$ (μM.h)	0.701 ± 0.087	5.86 ± 0.21*	3.95 ± 0.58	0.854 ± 0.278*
C_{max} (μM)	0.107 ± 0.011	0.333 ± 0.010*	0.369 ± 0.085	0.142 ± 0.058*
IV Cobimetinib				
$AUC_{(0\text{-}inf)}$ (μM.h)	1.01 ± 0.46	3.73 ± 0.93*	-	-
CL (mL/min/kg)	34.8 ± 12.5	8.71 ± 2.01*	-	-
$T_{1/2}$ (hr)	5.09 ± 1.93	22.5 ± 6.6*	-	-

$Cyp3a^{-/-}$Tg-$3A4_{Hep/Int}$ – liver and intestinal expression of CYP3A4
* $P<0.05$ compared to corresponding control animals

DMD Fast Forward. Published on March 26, 2015 as DOI: 10.1124/dmd.115.063743
This article has not been copyedited and formatted. The final version may differ from this version.

Table 3: Exposure (AUC and C_{max}; Mean ± SD) of cobimetinib in FVB (WT) and Cyp3a (-/-) mice with and without treatment with itraconazole

	FVB		Cyp3a (-/-)	
	No Treatment	Itraconazole	No Treatment	Itaconazole
PO Cobimetinib				
$AUC_{(0\text{-tlast})}$ (μM.h)	1.38 ± 0.25	8.03 ± 1.06*	6.42 ± 1.07	10.7 ± 2.9
C_{max} (μM)	0.175 ± 0.041	0.509 ± 0.065*	0.479 ± 0.077	0.644 ± 0.355

n= 3-6 mice/group; *p<0.05 compared to corresponding control animals

Figure 1

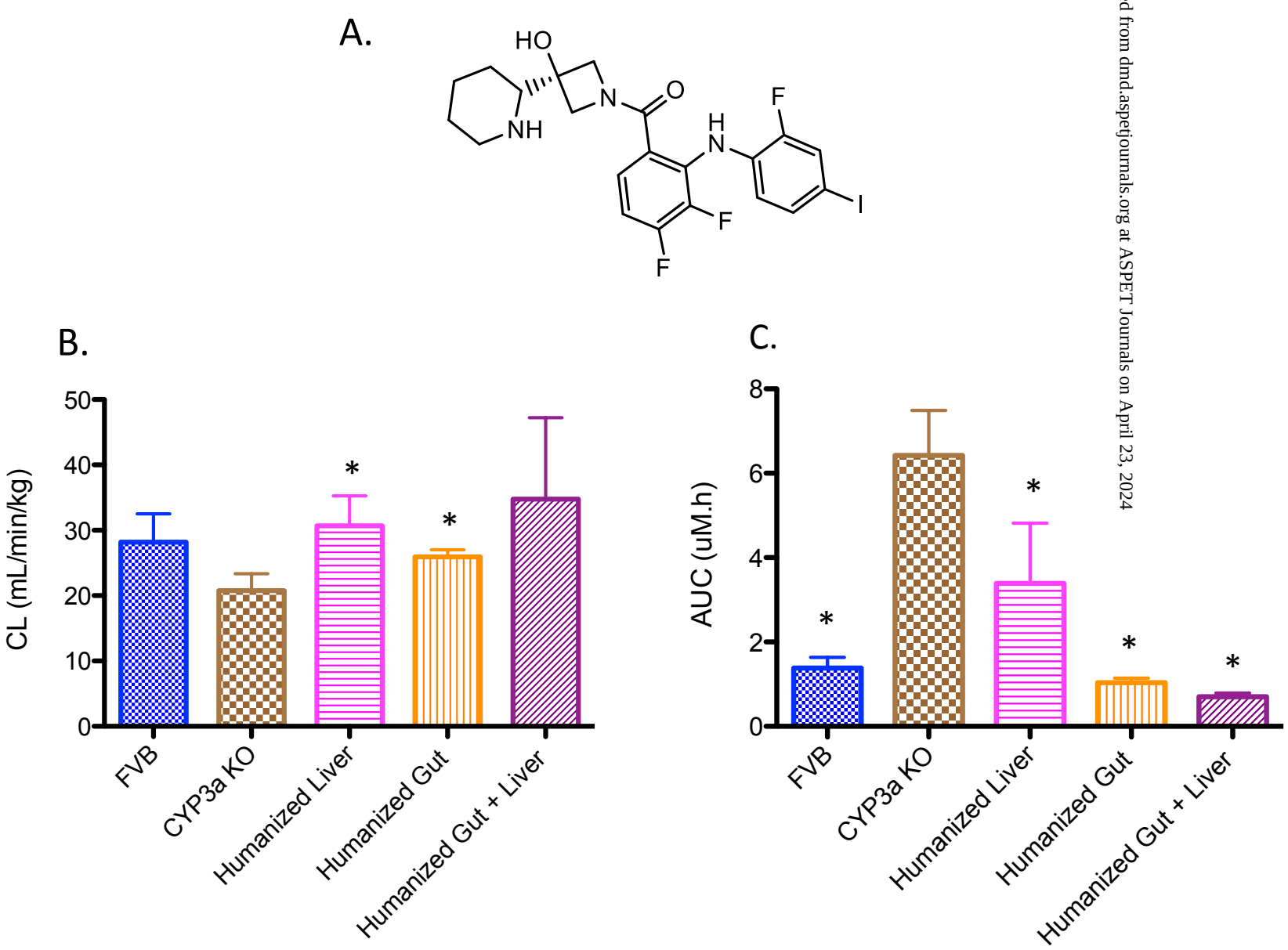

* p<0.05; compared to Cyp3a KO

Figure 2